Theories of rotary motors

Richard M. Berry

The Randall Institute, King's College London, 26–29 Drury Lane, London WC2B 5RL, UK

The bacterial flagellar motor and the ATP-hydrolysing F_1 portion of the F_1F_o-ATPase are known to be rotary motors, and it seems highly probable that the H^+-translocating F_o portion rotates too. The energy source in the case of F_o and the flagellar motor is the flow of ions, either H^+ (protons) or Na^+, down an electrochemical gradient across a membrane. The fact that ions flow in a particular direction through a well-defined structure in these motors invites the possibility of a type of mechanism based on geometric constraints between the rotor position and the paths of ions flowing through the motor. The two best-studied examples of such a mechanism are the 'turnstile' model of Khan and Berg and the 'proton turbine' model of Läuger or Berry. Models such as these are typically represented by a small number of kinetic states and certain allowed transitions between them. This allows the calculation of predictions of motor behaviour and establishes a dialogue between models and experimental results. In the near future structural data and observations of single-molecule events should help to determine the nature of the mechanism of rotary motors, while motor models must be developed that can adequately explain the measured relationships between torque and speed in the flagellar motor.

Keywords: bacterial flagella; F_oF_1-ATPase; molecular motors; protein machines

1. INTRODUCTION

Nature has not made much use of the wheel. Bacterial flagella are the only biological structures known that use rotation for the purpose of locomotion (Macnab 1996; Berry & Armitage 1999). Flagella consist of a rotary motor embedded in the cell envelope connected to an extracellular helical propeller. The motor is powered by the flow of ions down an electrochemical gradient across the cytoplasmic membrane into the cell. The ions are typically H^+ (protons), although certain marine and alkalophilic species have motors driven by Na^+. The electrochemical gradient ('protonmotive force' or 'sodium-motive force') consists of a transmembrane voltage and a concentration difference across the membrane, both of which are maintained by various metabolic processes. Figure 1a shows the structure of the flagellar motor (Coulton & Murray 1978; Francis *et al.* 1989). The rotor, shown in white, consists of a series of rings spanning the cell envelope and is attached via the flexible hook to the helical propeller, or 'filament'. The stator is a ring of particles in the cytoplasmic membrane, containing the proteins MotA and MotB, and anchored to the peptidoglycan cell wall. When compared with the ATP-driven linear motors of eukaryotes the performance of the flagellar motor is impressive. Single MotA/MotB units in *Escherichia coli* can generate over 300 pN nm of torque (Ryu *et al.* 2000), and the Na^+-driven motors of *Vibrio alginolyticus* can rotate at up to 1700 Hz (Magariyama *et al.* 1994). Translated into linear forces and velocities at the perimeter of the rotor, these become approximately 15 pN and approximately 200 µm s^{-1}, respectively. By comparison, single kinesin molecules moving on microtubules can generate 5–6 pN of force and move at 1 µm s^{-1}, while myosin molecules exert forces up to about 6 pN upon actin filaments, and even in large arrays in muscle fibres do not move much faster than 10 µm s^{-1}.

It is now known that the ATP-hydrolysing F_1 portion of the F_1F_o-ATPase is also a rotary motor (Noji *et al.* 1997), and it seems highly probable that the H^+-translocating (or Na^+-translocating in some species) F_o portion rotates too. The purpose of the F_1F_o-ATPase is to couple ATP hydrolysis in F_1 to proton flux across the membrane in F_o, and rotary motion is a means to this end rather than an end in itself. Nonetheless, the complex can be considered as two reversible rotary motors connected 'back-to-back' by a common rotor, such that rotation of F_o driven by proton flux leads to ATP production in F_1, while ATP hydrolysis in F_1 drives the rotor in the opposite direction and leads to proton pumping in F_o (Engelbrecht & Junge 1997; Junge *et al.* 1997). The structure of the F_1F_o-ATPase is shown in figure 1b (which is reproduced in figure 1a to show its size relative to the bacterial flagellar motor). The common rotor consists of the γ- and ϵ-subunits in F_1 connected to a ring of c-subunits in F_o. The stator in F_1, (the hexamer $\alpha_3\beta_3$) is connected to the stator in F_o, (a-subunit) by a linker containing the b- and δ-subunits. Rotation of F_1 driven by ATP hydrolysis has been observed directly by sticking the F_1 stator to a cover-slip and attaching fluorescent actin filaments to the γ-subunit (Noji *et al.* 1997). Rotation of F_o has never been observed directly.

A detailed model of the mechanism of the ATP-driven F_1 rotary motor has been published (Wang & Oster 1998) but will not be discussed here. Instead we will focus on models of the mechanism of rotary motors driven by the flux of ions across a membrane. These models have been formulated with the bacterial flagellar motor in mind, but the same principles can be and have been applied to the F_o motor (Oosawa & Hayashi 1986; Vik & Antonio
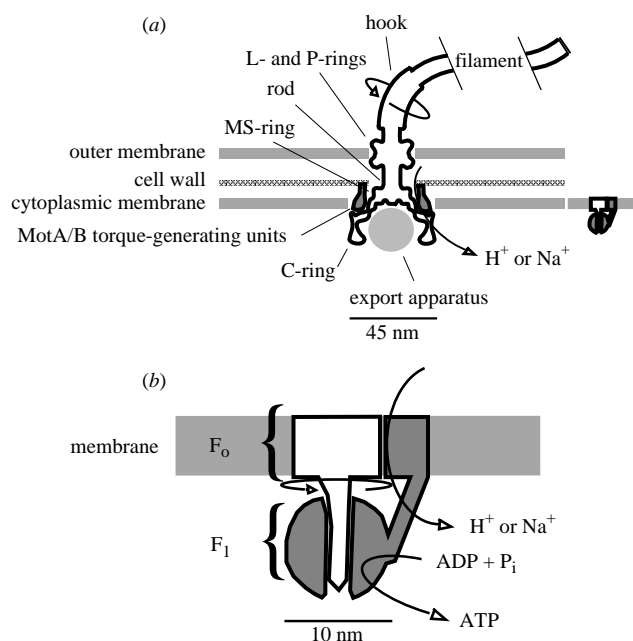
503

(a)

(b)

Figure 1. Structures of biological rotary motors. (*a*) The bacterial flagellar motor. The rotor, drawn in white, consists of a series of rings that span the cell envelope and are attached to the extracellular hook and filament. The stator consists of a ring of torque-generating units containing the proteins MotA and MotB and anchored to the cell wall. (In Na^+-driven flagellar motors the proteins involved are PomA and PomB, analogues of MotA and MotB, and the additional proteins MotX and MotY.) Ions flowing through the motor generate torque by means of unknown interactions between the rotor and stator in the vicinity of the C-ring. The F_oF_1-ATPase is also shown, to the same scale. (*b*) The F_oF_1-ATPase contains two rotary motors; the membrane-bound F_o, driven by the flux of ions across a membrane, and the soluble F_1, driven by ATP hydrolysis. These two motors are coupled by sharing a common rotor, drawn in white, and a common stator, drawn dark. The figure shows the F_oF_1-ATPase operating as an ATP-synthase. Rotation of F_o driven by ion flux drives F_1 in reverse, causing it to synthesize ATP from ADP and inorganic phosphate.

1994; Elston *et al*. 1998). Both motors are found in H^+- and Na^+-driven forms with similar structural and functional properties, and functional chimeric motors have been constructed combining parts from H^+- and Na^+-driven forms (Asai *et al*. 1999). This indicates that the mechanism is similar for the two ionic species, and while we will generally discuss H^+-driven motors, discussions will be assumed to apply equally to Na^+-driven motors.

2. PHYSICAL MODELS OF ROTARY MOTORS

In both F_o and the flagellar motor the rotor and stator are held together in a well-defined structure, and rotation is driven by the flow of ions in a particular direction through this structure. By contrast, motor molecules such as kinesin can bind to microtubules and move along them in the absence of any other structural elements, and the process of ATP hydrolysis that drives these motors is not associated with any inherent direction. The vectorial nature of the driving force in the flagellar

motor does not rule out a mechanism of the type generally accepted for linear, ATP-driven motors. That is to say the mechanochemical cycle of the motor could consist of binding between rotor and stator, conformational changes driven by proton transit that exert torque upon the rotor, and subsequent unbinding and reversal of the conformational change to complete the cycle (see figure 2*a*). Such a model has been proposed by Läuger (1998), and it is possible that if single MotA/MotB units could be added to purified rotors in an energized membrane and observed, they would be seen to run around the rotor without the need for an anchor to the cell wall or any other structural elements. This experiment has never been attempted, however, and it is equally possible that the MotA/MotB units in such an arrangement would be unable to move. Such a result as this might point to an altogether different type of mechanism, based on geometric constraints between the rotor position and the paths of ions flowing through the motor. This type of mechanism is worth considering simply because it is possible. The structure, performance and driving force of the flagellar motor are different from those of ATP-driven motors. Perhaps the flagellar motor is able to generate so much torque and rotate so fast, despite the fact that the combined size of MotA and MotB is about half that of a single myosin head, by taking advantage of a mechanism that depends upon using the electrochemical proton gradient directly.

The two best-studied examples of such a mechanism are the 'turnstile' model of Khan & Berg (1983; Meister *et al*. 1989) and the 'proton turbine' model of Läuger (Läuger 1977, 1988; Kleutsch & Läuger 1990) or Berry (1993). The turnstile model is illustrated in figure 2*b*. Protons from outside the cell are deposited onto the rotor by one type of ion channel in a stator unit, and are carried by diffusion of the rotor to a second type of ion channel on the stator unit that allows them to pass into the cell, completing the motor cycle. Unless it is protonated, the rotor is bound to a stator unit and unable to move between the two types of channel. This constraint combined with the path that ions take through the motor ensures that rotation and ion transit are tightly coupled. The physical nature of the constraint was not specified in the original model, but in variations on the same theme (Blair 1990) and an adaptation of the model applied to F_o (Elston *et al*. 1998) it is assumed to arise from electrostatic forces between charges on the rotor and stator and from the high energy cost of exposing charges on the rotor to the low dielectric constant of the membrane.

Another feature of the model of Khan & Berg (1983) is an elastic link between the stator unit and the cell wall. Without this, rotation of the motor would be limited by diffusion of the entire rotor, once protonated, between the two types of channel. By stretching the elastic link the stator unit (much smaller and therefore diffusionally faster than the rotor) can diffuse around the rotor, bind to the rotor by allowing the proton to pass into the cell, and then exert torque upon the rotor via the stretched link. In either case, the model relies upon thermal fluctuations to carry the rotor and the stator unit past each other to the point where the proton can pass into the cell. The model is a 'thermal ratchet', in that the role of the free energy supplied by the influx of protons is to 'save' thermal
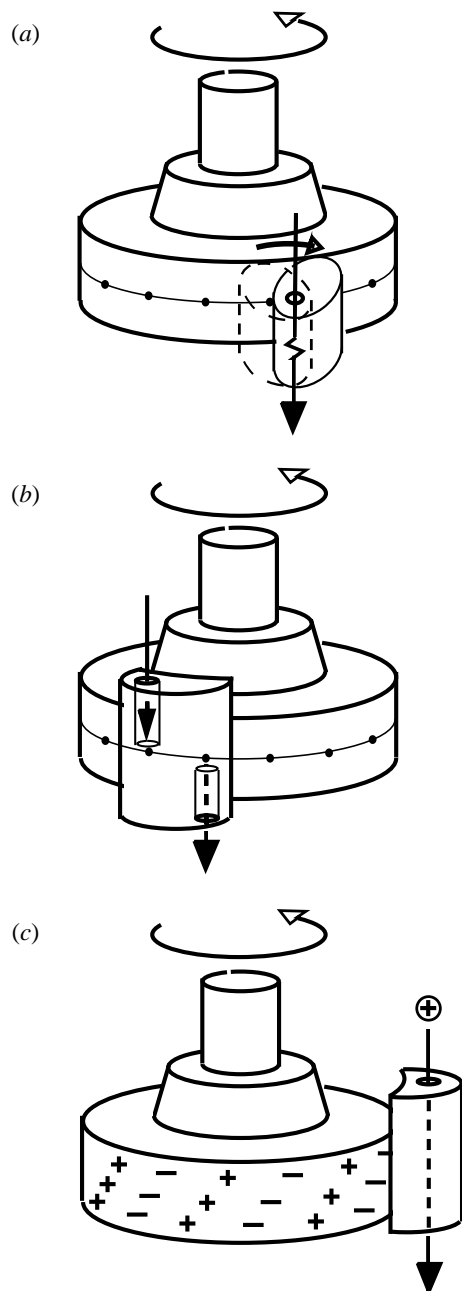
Figure 2. Possible mechanisms for ion-driven rotary motors.
(*a*) Torque is generated by the following mechanical cycle.
(i) The stator unit binds the rotor in the conformation
marked by the dashed lines. (ii) A conformational change
to the conformation marked by the solid lines occurs,
generating torque via the attachment between the rotor
and stator. (iii) The stator unbinds from the rotor.
(iv) The stator returns to its original conformation,
completing the cycle. This mechanical cycle is coupled
to the influx of one or more protons through the stator
unit. (*b*) 'Turnstile'. Ions are deposited onto the rotor
by channels that extend to the outside of the cell (top),
and are removed by separate channels that extend into
the cytoplasm (bottom). To pass into the cell, ions must
be carried from one type of channel to the other by rotation
of the rotor. (*c*) 'Proton turbine'. Positively charged ions
flowing through the stator attract lines of negative charges
and/or repel lines of positive charges on the rotor. These
electrostatic forces keep the line of negative charges close to
the ion as it passes into the cell, which leads to rotation if the
lines of charge on the rotor are tilted relative to the ion
channel in the stator.

fluctuations in a certain direction rather than to create
directly a torque-generating state.

Figure 2*c* illustrates the proton turbine model of Berry
(1993). The key elements in this type of model are low
energy paths for ions on both stator and rotor that are
tilted with respect to each other. Ions can only cross the
membrane if they remain at the intersection of a path on
the rotor and another on the stator. For the intersection
point carrying an ion to pass from one side of the
membrane to the other the rotor must rotate, so rotation
and ion flux are coupled. In the model of Berry (1993),
ions travel through channels on the stator, and the
complementary tilted 'paths' on the rotor are alternating
lines of positive and negative charges. Positively charged
ions in the channel will attract lines of negative charges
by long-range electrostatic interactions. The force
between two unit charges separated by 6 Å in a medium
of relative dielectric constant 5 (typical of a protein
interior) is 130 pN, which is more than enough to account
for the torque that the motor generates. The structure of
the rotor is not known in sufficient detail to say whether
such lines of charges exist. However, site-directed
mutagenesis of both rotor and stator proteins has shown
that various charged residues are important for motor
function, that it is the charge of these groups rather than
the specific residue that is important, and that removal or
reversal of most of the charges individually impairs but
does not destroy motor function (Lloyd & Blair 1997;
Zhou & Blair 1997; Zhou *et al.* 1998). This evidence is
consistent with a model where the motor generates torque
via long-range electrostatic interactions.

In the model of Oosawa & Hayashi (1983, 1986)
protons cross the membrane by binding to a mobile
carrier attached to the stator, rather than by flowing
through stator channels. Torque generation is not expli-
citly electrostatic in nature, but derives from the force of
binding between the protonated carrier and tilted pairs of
sites on the rotor. Apart from these differences, the model
is similar to the proton turbine model of Berry.

In the model of Läuger (1977, 1988; Kleutsch & Läuger
1990), the tilted paths on rotor and stator are described as
'half-channels'. Each is assumed to lower the energy of an
associated ion crossing the membrane, but not enough to
compensate for the energy needed to remove the ion from
aqueous solution. Only when an ion is associated with
rotor and stator half-channels simultaneously can it cross
the membrane. It was envisaged that both sets of half-
channels would be situated at the rotor–stator interface
and that protons would cross the membrane in close
contact with them. With a proton a certain fraction of the
way through the membrane, the rotor is assumed to be
bound to the stator at a fixed position such that the two
half-channels intersect at the proton.

As in the turnstile model of Khan & Berg, the stator
half-channels in the model of Läuger are assumed to be
attached to the cell wall via elastic linkages. The key
difference between the two models is in the path that
protons take through the motor. In the turnstile model,
proton transit across the membrane and rotation of the
rotor occur in separate steps, while in the proton turbine
model, they occur simultaneously. The proton turbine
model is a 'power stroke' mechanism, in that the free
energy supplied by the influx of protons is directly

coupled to the creation of a torque-generating state, and thermal fluctuations are not necessary for rotation to occur. This is best seen in the electrostatic version of the model, illustrated in figure 2c. The membrane voltage drives protons further towards the inside of the cell, and also further away from the line of negative charges on the rotor. This directly generates torque in the form of the electrostatic attraction between the proton and these charges and the repulsion between the proton and the adjacent line of positive charges.

The distinction between ratchet-like turnstile models and power-stroke-like turbine models can be blurred. For example, the model of Dimroth *et al.* (1999) for a Na⁺-driven F₀ motor is structurally a variant on the turnstile model. However, it assumes that the entire transmembrane voltage appears tangentially at the interface between the rotor and the stator unit. This means that upon binding a sodium ion the rotor is driven by electrostatic forces towards angles where the ion can pass through to the cytoplasm, rather than having to get there by thermal fluctuation alone. Thus the mechanism is somewhere between a power stroke and a thermal ratchet.

Many other models for the mechanisms of rotary motors have been published. For a summary of flagellar motor models see Berg & Turner (1993) or Berry & Armitage (1999). I have focused on the turnstile and proton turbine models partly because they are the best-studied models of the flagellar motor, but also because they are representative of the two most common recurring themes in models of rotary motors driven by the flux of ions across a membrane.

3. MATHEMATICAL TREATMENT OF MOTOR MODELS

A physical model of a rotary motor must be consistent with known facts about the structure of the motor. When new structural details emerge that are at odds with a particular model, the model must either be abandoned or modified to take them into account. To distinguish between models that are consistent with structural data requires a mathematical treatment of the models leading to predictions of how the motor should behave under various experimentally accessible conditions. A model motor can be represented by several key variables. In a flagellar motor model the angle between reference points on the rotor and stator and the three coordinates of the position of a transient proton are obvious choices. Conformational changes of motor proteins can be reduced to a small number of variables; for example the relative translation of two domains, the tilt angle about a certain hinge point, the bending or stretching of elastic elements. Even at this level, however, the model exists in a complex multidimensional space. To specify the equations of motion in such a space, and to calculate from them the behaviour of the motor, presents a daunting computational challenge.

The next level of simplification is to assume that the model spends most of its time in a few particular regions of the entire model space, and to represent these regions by discrete kinetic states. The dynamics of the model are then represented by a set of permitted transitions between these states. The choice of states and transitions between
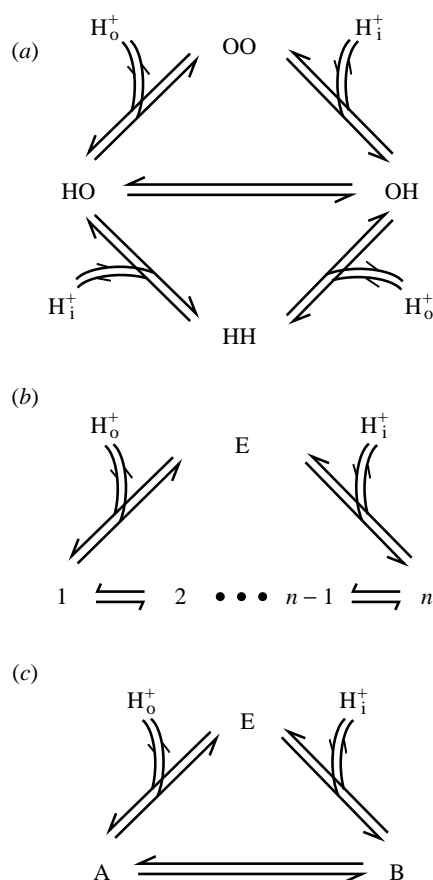

Figure 3. Kinetic representations of motor models. (*a*) The 'turnstile' model of Khan & Berg (figure 2*b*). The state OO represents the motor with no ions bound to the rotor, in which case the rotor is assumed to be unable to rotate relative to the stator. Uptake of a proton from the outside (H_o^+) leads to state HO, in which a proton is bound to the rotor near an external channel. With a proton bound, the rotor can rotate and carry the proton to the internal channel, denoted by the transition to state OH. From there, the proton can pass into the cell, returning the motor to state OO. An alternative cycle exists, in which protons are bound to the rotor near to both internal and external channels, a state denoted by HH. This cycle couples the influx of protons to rotation in the same direction as the cycle above. (*b*) The half-channel–turbine model of Läuger. State E represents the motor with no ions bound, states 1 to *n* represent the motor with a proton at one of *n* sites comprising an ion channel through the motor. The angle of the rotor in each of these states is such that the half-channels on the rotor intersect those on the stator at the position of the proton. One anticlockwise cycle couples the transit of a single proton to rotation of the rotor through the angle between the two ends of a rotor half-channel. (*c*) A simplified kinetic diagram with no particular physical interpretation. Transitions between state E and states A or B represent the exchange of protons with the solutions on either side of the membrane, all other movements of the motor are summarized in the transition between states A and B. By distributing proton transit and rotation between these three transitions according to free parameters of the model, certain features of the experimental relationship between torque and speed in the flagellar motor can be predicted.

them is often self-evident from the physical description of the model. In the simplest type of treatment all variables, including the rotor–stator angle, are represented by a few kinetic states. For example, figure 3a shows the kinetic

diagram for the turnstile model of Khan & Berg (Meister *et al*. 1989). State OO represents the stator unit bound to a particular pair of sites on the unprotonated rotor. The binding to the rotor of a proton from outside the cell, via the first type of channel, moves the model into state HO. The transition from state HO to state OH represents relative motions of the rotor and stator that carry the proton to the second type of channel, and the cycle is completed by the passage of the proton into the cell, represented by the transition back to state OO. The doubly protonated state HH takes part in a similar cycle that also couples the influx of one proton to a rotation through the angle separating the two types of channel. Figure 3*b* shows the kinetic diagram for the turbine model of Läuger (1988). The half-channels are assumed to consist of a chain of n distinct proton-binding sites. Site 1 exchanges protons with the outside of the cell, site n exchanges protons with the inside, and all other transitions represent transfer of protons between adjacent sites simultaneous with relative rotation of the rotor and stator unit.

These models are inherently 'tight-coupled', since rotation and proton transit are bundled together into single kinetic transitions. (Variable stoichiometry can be accommodated by adding alternative 'uncoupled' cycles to the kinetic diagram that represent either rotation or proton transit without the other.) Predictions of the relationship between torque, protonmotive force and speed in the motor are obtained in the following way. Rate constants for the kinetic transitions are calculated at specified values of load torque, transmembrane voltage, and internal and external ion concentrations. From these rate constants the steady-state occupancies of the kinetic states are calculated, and the net rate of the motor cycle is given by the net flux between any two states in the cycle. Because of the tight-coupling constraints, the rotation speed is simply equal to the product of the cycle rate and the angle moved per cycle. Load torque will affect the rate constants of any transitions that involve rotation, via a work term in the free energy difference between the initial and final states (equal to the product of the torque and the rotation angle). Similarly, the transmembrane voltage will affect the rates of any transitions where charged ions move through some fraction of this voltage, and the ion concentrations will affect the rates of transitions that incorporate the uptake of ions from either side of the membrane.

The kinetic diagrams in figure 3*a,b* are not so very different. If state HH in figure 3*a* has vanishingly low occupancy, and if $n = 2$ in figure 3*b*, then they are identical. The only remaining difference between the kinetic representations of the turnstile and turbine models lies in the values of the rate constants, and the way in which they depend upon membrane voltage and torque. However, as discussed earlier, these things are not always sufficiently constrained by the structural description of a model to distinguish between structurally different models. In the case of F_o and the flagellar motor, the current lack of detailed structural information provides rather few constraints on possible mechanisms. (For example, in a typical turnstile model the step denoted by HO→OH in figure 3*b* is unaffected by the membrane voltage; but in their model of F_o, Dimroth *et al*. (1999) were free to assume that this step does in fact depend on
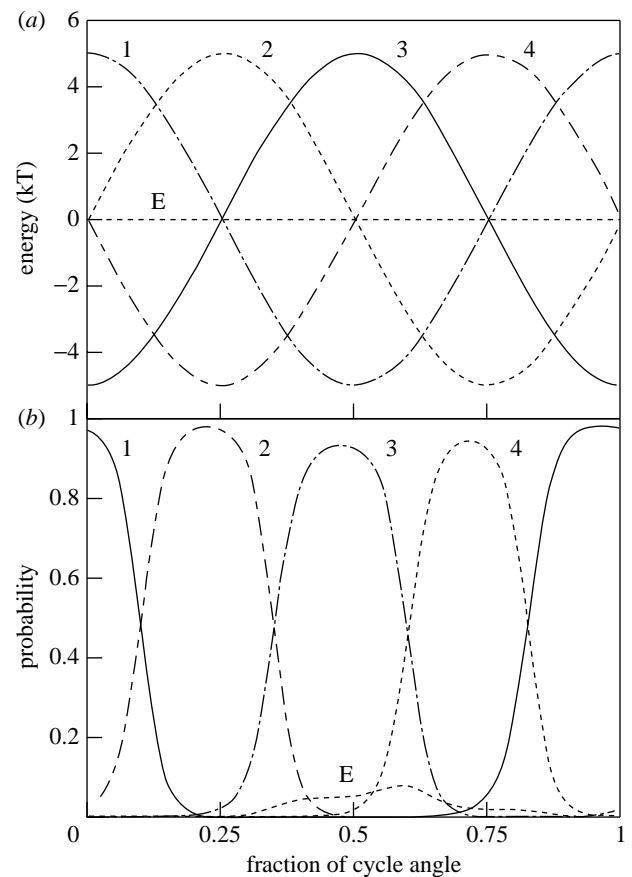

Figure 4. 'Loose-coupled' treatment of a motor model. (*a*) Electrostatic energies of the motor with ions at four equally spaced sites in the stator channels of the model of Berry (1993), as a function of the rotor–stator angle. These energies arise from long-range electrostatic interactions between the ion in the channel and alternating lines of positive and negative charges on the rotor. (*b*) The probability that each state is occupied as a function of angle, with the rotor stationary and a transmembrane voltage of −150mV. Each state is occupied predominantly at angles where the torque, equal to minus the derivative of energy with respect to angle, is positive.

the membrane voltage in order to explain certain experimental observations.) On the other hand, there is a growing body of data on the performance of the flagellar motor, in particular the relationships between torque, speed and protonmotive force (Berry & Armitage 1999; Berg, this issue). Figure 3*c* shows a minimal kinetic diagram which does not correspond to any particular physical model (Berry & Berg 1999). Transitions between states E and A or B represent the exchange of protons with the outside or inside of the cell, respectively, and all events that occur while protons are inside the motor are summarized by a single transition between states A and B. The rate constants and the way in which they depend upon torque and membrane voltage are free parameters of the model. After adjusting these parameters to match the experimental data, it is then possible to interpret the 'best-fit' parameters in terms of constraints upon possible underlying physical mechanisms. For example, in the context of a tight-coupled model with the kinetic diagram of figure 3*c*, the concave-down dependence of torque upon speed (Berg & Turner 1993) in the flagellar motor

requires a power stroke mechanism, while the continuity of torque through zero speed prohibits any mechanism that contains a step that is essentially irreversible and insensitive to external torque (Berry & Berg 1999).

Kinetic models are useful in interpreting experimental data such as the torque–speed relationship, and in providing insights into the key features of the mechanism of rotary motors. However, these insights are only as good as the assumptions of the model. In particular, it is possible that the bundling together of rotation with all the other internal processes of the motor into a few kinetic transitions might miss some crucial feature of the mechanism. An alternative modelling strategy is to allow the slowest process (assumed to be rotor rotation) to be continuously variable while other processes are represented by reaction kinetics as before. The kinetic rate constants become functions of rotor angle, as do the torques exerted upon the rotor in each kinetic state. This type of treatment was used in early models of muscle contraction (Huxley 1957; Huxley & Simmons 1971) and also in the flagellar motor models of Oosawa & Hayashi (1983, 1986) and Berry (1993). The latter models assume a constant rotation rate, and use the steady-state occupancy probabilities of the different states at different angles to calculate the average torque generated by the motor and the proton flux. For example, figure 4*a* shows the electrostatic energies of kinetic states in the model of Berry (1993) as a function of the rotor–stator angle. The stator ion channel is assumed to consist of four proton-binding sites spaced out equally across the trans-membrane voltage, and the kinetic diagram at each angle is the same as that of figure 3*b* with $n = 4$. At zero speed and with a transmembrane voltage of -150 mV, each state is most likely to be occupied at angles just below its energy minimum (figure 4*b*). The torque generated by the motor in each state is equal to minus the derivative of energy with respect to angle, and the average torque is positive because of the voltage-induced shift of state occupancies to the left of the energy minima of each state.

More recent models of F_o and the flagellar motor (Elston *et al*. 1998; Elston & Oster 1997; Dimroth *et al*. 1999) dispense with the assumption of constant torque. Monte Carlo simulations of the equation of motion of the rotor coupled with the allowed kinetic transitions are used to obtain predicted trajectories of the motor, while state occupancies, averaged torques and speeds can be found by numerical solution of the associated reaction diffusion equations.

This 'mixed' approach is more realistic than the pure kinetic treatments discussed above, and allows sophisticated predictions of motor behaviour to be made. In the future, when structural data and experimental techniques allow energy profiles and rate constants in rotary motors to be calculated or measured, such descriptions of motor models may provide a full and detailed understanding of the motor mechanism. In the meantime, however, energy profiles and rate constants must be educated guesses at best, and the role of models is to explore possible mechanisms and suggest which are the important quantities to measure. The role of experiments is to provide data to support some models and rule out others, and perhaps occasionally to suggest a whole new class of model. For the F_o and F_1 rotary motors the ball is in the experiment-alists' court; to make direct observations of rotation in F_o and measurements of the relation between torque and speed in F_1 to confirm or confound the detailed predictions of recent models. In both F_o and the flagellar motor more detailed structural information is urgently needed. For the flagellar motor, experiments to observe events at the single-molecule level need to be done in order to narrow the range of possible models. In the meantime modellers face the challenge of adequately explaining the measured relationship between torque and speed in the motor.

REFERENCES

Asai, Y., Kawagishi, I., Sockett, R. E. & Homma, M. 1999 Hybrid motor with H^+ and Na^+-driven components can rotate *Vibrio* polar flagella by using sodium ions. *J. Bacteriol.* **181**, 6332–6338.

Berg, H. C. & Turner, L. 1993 Torque generated by the flagellar motor of *Escherichia coli*. *Biophys. J.* **65**, 2201–2216.

Berry, R. M. 1993 Torque and switching in the bacterial flagellar motor: an electrostatic model. *Biophys. J.* **64**, 961–973.

Berry, R. M. & Armitage, J. P. 1999 The bacterial flagellar motor. *Adv. Microb. Physiol.* **41**, 291–337.

Berry, R. M. & Berg, H. C. 1999 Torque generated by the flagellar motor of *Escherichia coli* while driven backward. *Biophys. J.* **76**, 580–587.

Blair, D. F. 1990 The bacterial flagellar motor. *Semin. Cell Biol.* **1**, 75–85.

Coulton, J. W. & Murray, R. G. E. 1978 Cell envelope associations of *Aquaspirillum serpens* flagella. *J. Bacteriol.* **136**, 1037–1049.

Dimroth, P., Wang, H., Grabe, M. & Oster, G. 1999 Energy transduction in the sodium F-ATPase of *Propionigenium modestum*. *Proc. Natl Acad. Sci. USA* **96**, 4924–4929.

Elston, T. C. & Oster, G. 1997 Protein turbines. I. The bacterial flagellar motor. *Biophys. J.* **73**, 703–721.

Elston, T., Wang, H. & Oster, G. 1998 Energy transduction in ATP synthase. *Nature* **391**, 510–513.

Engelbrecht, S. & Junge, W. 1997 ATP synthase: a tentative structural model. *FEBS Lett.* **414**, 485–491.

Francis, N. R., Sosinsky, G. E., Thomas, D. & De Rosier, D. J. 1989 Isolation, characterisation and structure of bacterial flagellar motors containing the switch complex. *J. Mol. Biol.* **345**, 1261–1270.

Huxley, A. F. 1957 Muscle structure and theories of contraction. *Prog. Biophys. Biophys. Chem.* **7**, 255–318.

Huxley, A. F. & Simmons, R. M. 1971 Proposed mechanism of force generation in striated muscle. *Nature* **233**, 533–538.

Junge, W., Lill, H. & Engelbrecht, S. 1997 ATP synthase: an electro-chemical transducer with rotary mechanics. *Trends Biochem. Sci.* **22**, 420–423.

Khan, S. & Berg, H. C. 1983 Isotope and thermal effects in chemiosmotic coupling to the flagellar motor of *Streptococcus*. *Cell* **32**, 913–919.

Kleutsch, B. & Läuger, P. 1990 Coupling of proton flow and rotation in the bacterial flagellar motor: stochastic simulation of a microscopic model. *Eur. Biophys. J.* **18**, 175–191.

Läuger, P. 1977 Ion transport and the rotation of bacterial flagella. *Nature* **268**, 360–361.

Läuger, P. 1988 Torque and rotation rate of the flagellar motor. *Biophys. J.* **53**, 53–65.

Lloyd, S. A. & Blair, D. F. 1997 Charged residues of the rotor protein FliG essential for torque generation in the flagellar motor of *Escherichia coli*. *J. Mol. Biol.* **266**, 733–744.

Macnab, R. M. 1996 Flagella and motility. In Escherichia coli *and* Salmonella: *cellular and molecular biology* (ed. F. C. Neidhardt, R. Curtiss, I. J. L. Ingraham, E. C. C. Lin, G. Lowe, B. Magasanik, W. S. Reznikoff, M. Riley, M. Schaechter & H. E. Umbarger), pp. 123–145. Washington, DC: American Society for Microbiology.

Magariyama, Y., Sugiyama, S., Muramoto, K., Maekawa, Y., Kawagishi, I., Imae, Y. & Kudo, S. 1994 Very fast flagellar rotation. *Nature* **371**, 752.

Meister, M., Caplan, S. R. & Berg, H. C. 1989 Dynamics of a tightly coupled mechanism for flagellar rotation. *Biophys. J.* **55**, 905–914.

Noji, H., Yasuda, R., Yoshida, M. & Kinosita, K. 1997 Direct observation of the rotation of F_1-ATPase. *Nature* **386**, 299–302.

Oosawa, F. & Hayashi, S. 1983 Coupling between flagellar motor rotation and proton flux in bacteria. *J. Physiol. Soc. Jpn* **52**, 4019–4028.

Oosawa, F. & Hayashi, S. 1986 The loose coupling mechanism in molecular machines of living cells. *Adv. Biophys.* **22**, 151–183.

Ryu, W. S., Berry, R. M. & Berg, H. C. 2000 Torque generating units of the flagellar motor of *Escherichia coli* have a high duty ratio. *Nature* **403**, 444–447.

Vik, S. B. & Antonio, B. J. 1994 A mechanism of proton translocation by F_1F_o ATP synthases suggested by double mutants of the α subunit. *J. Biol. Chem.* **269**, 30 364–30 369.

Wang, H. & Oster, G. 1998 Energy transduction in the F_1 motor of ATP synthase. *Nature* **396**, 279–282.

Zhou, J. & Blair, D. F. 1997 Residues of the cytoplasmic domain of MotA essential for torque generation in the bacterial flagellar motor. *J. Mol. Biol.* **273**, 428–439.

Zhou, J., Lloyd, S. A. & Blair, D. F. 1998 Electrostatic interactions between rotor and stator in the bacterial flagellar motor. *Proc. Natl Acad. Sci. USA* **95**, 6436–6441.